Temperature and strain rate sensitivity of shocked aluminium: multiscale dislocation dynamics simulations

Abdo Hamieh, Samir Mustapha and Mutasem Shehadeh*

Mechanical Engineering Department,
American University of Beirut,
Beirut, 11072020, Lebanon
Email: amh52@mail.aub.edu
Email: sm154@aub.edu.lb
Email: ms144@aub.edu.lb
*Corresponding author

Abstract: Multiscale dislocation dynamics plasticity (MDDP) simulations are carried out to investigate the mechanical response of aluminium single crystals subjected to extreme conditions of high strain rate over a wide range of temperatures. Atomistically informed generalised dislocation mobility law is integrated in MDDP and the effects of temperature and strain rate on the dynamic yield point are scrutinised. Additionally, pressure and temperature-dependent elastic properties are employed to better capture the shockwave characteristics under thermochemical extreme conditions. The simulation results reveal unusual thermal hardening effect along with strain rate hardening behaviour. Based on the simulations findings, physically-based constitutive equation for the dynamic yield strength is proposed.

Keywords: dislocation dynamics; shockwave; high strain rate; nucleation; multiscale simulation.

Reference to this paper should be made as follows: Hamieh, A., Mustapha, S. and Shehadeh, M. (2021) 'Temperature and strain rate sensitivity of shocked aluminium: multiscale dislocation dynamics simulations', *Int. J. Theoretical and Applied Multiscale Mechanics*, Vol. 3, No. 4, pp.363–375.

Biographical notes: Abdo Hamieh is a former graduate student in the Mechanical Engineering Department at the American University of Beirut. His research interests are in the area of numerical modelling of the mechanical response of crystalline materials.

Samir Mustapha has an undergraduate degree in Aeronautical Engineering and a PhD in Engineering from the University of Sydney in 2013. He joined the American University of Beirut in 2014 as a Professor in Mechanical Engineering. His research interests include materials science, sensing systems, numerical modelling, and data analytics.

Mutasem Shehadeh is an Associate Professor of Mechanical Engineering at the American University of Beirut (AUB). Prior to joining AUB in 2008, he was a Visiting Assistant Professor at the Villanova University, PA. He obtained his PhD in Mechanical Engineering from the Washington State University in 2005, MS and BS in Mechanical Engineering from the University of Jordan in 2000

and 1998, respectively. His research is centred on the development and application of predictive simulation tools to understand the deformation mechanisms in engineering materials with particular interest on understanding the materials' behaviour under high strain rate deformations.

1 Introduction

The mechanical response of FCC metals subjected to shock compression at elevated temperature has recently attracted the attention of many research groups. Experiments (Kanel, 2012, Zaretsky and Kanel, 2017; Yanilkin et al., 2014; Gurrutxaga-Lerma et al., 2017) and numerical simulations via molecular dynamics (Tramontina et al., 2014; Agarwal et al., 2020) and discrete dislocation dynamics (Shehadeh et al., 2006; Shehadeh, 2012; Gurrutxaga-Lerma et al., 2015b) have been carried out to investigate fundamental aspects of shock-induced plasticity in metals. While most of the published work has focused on understanding the microstructure and the dislocation mechanisms at room temperature, it is expected that when a high rate of deformation is accompanied by elevated temperature, the mechanical response of the material is no longer determined by the applied stress but also by the high temperature that may affect the overall response of the materials (Kanel et al., 2000, 2001; Kanel and Razorenov, 2001; Kanel, 2012). In this case, the dislocation motion is dominated by dislocation drag and not by thermal activation and the need to overcome the Peierls barrier.

It is well established, that plasticity in metals is controlled by the generation and motion of dislocations. For most metals subjected to low/moderate strain rate loadings, it is found that the yield point decreases with increasing temperature (Kanel et al., 2001; Choudhuri and Gupta, 2013; Gurrutxaga-Lerma et al., 2017). Under such conditions, it is thought that the dislocation motion is controlled by thermal activation process that assists dislocations in overcoming their local barriers, in this case, the Peierls barrier. This dislocation therefore can glide easily, at lowered levels of mechanical stress leading to the observed drop in the yield point this will result in the plastic flow, thus the yield point drops (Shehadeh and Zbib, 2016).

However, under high/ultra-high strain rate loading, this temperature softening effect is not observed, to the contrary, in shock experiments of FCC metals such as aluminium, thermal hardening is observed (Kanel, 2012). This thermal hardening effect under shock compression may be rationalised by accounting for the competing factors of temperature-dependent elastic properties, and the temperature and strain rate dependent drag that opposes the dislocation glide. It is now widely accepted that as the rate of deformation increases, the process of deformation becomes increasingly drag controlled (Hirth et al., 1998; Hirth and Lothe, 1982; Armstrong and Walley, 2008). Under shock conditions, the level of stress can easily exceed the Peierls barrier and probably the ideal strength of the material. This results in accelerating the dislocations to a velocity approaching the shear wave speed. In this case, the dislocation motion is dominated by dislocation drag and not thermal activation. In addition to the velocity of the dislocations, the drag coefficient is affected by the deformation temperature as a result of phonon scattering and phonon wind effects (Olmsted et al., 2005). This resistance is proportional to temperature, i.e., when temperature increases, the drag increases, and the dislocation motion is hindered.

Gurrutxaga-Lerma et al. (2013) developed a fully time-dependent elastodynamic description of the elastic fields of discrete dislocations which is used to provide full explanation of 'the decay of the elastic precursor'. It turns out that this decay results from the interference of the elastic shock wave with elastic waves produced from the nucleated dislocations in the shock front (Gurrutxaga-Lerma et al., 2015a, 2017; Cui et al., 2019). Moreover, Kattoura and Shehadeh (2014) carried out multiscale dislocation dynamics simulations to investigate the mechanical response of copper single crystals under shock loading. Plasticity mechanisms associated with source activation and homogeneous nucleation of glide loops are considered for samples subjected to high strain rates ranging between 10^6 and 10^{10} s^{-1}.

This work focuses on investigating the mechanical response of aluminium single crystals subjected to shock compression over a wide range of temperatures (between 125 K to 605 K). The effects of strain rate and deformation temperature on the dynamic yielding behaviour are discussed. In the next section, the methodology and the simulation setup used in this work are described.

2 Methodology: multiscale dislocation dynamics plasticity

Multiscale dislocation dynamics plasticity (MDDP) (Zbib et al., 2003; Zbib and de la Rubia, 2002) is a multiscale elasto-viscoplastic simulation model in which three-dimensional discrete dislocation dynamics (DDD) is coupled with continuum finite element analysis (FEA). In the nano-microscale, isotropic elasticity DDD computations are used to determine the plasticity of single crystals by explicit three-dimensional evaluations of dislocations motion and interaction among themselves and other defects. The dislocations are discretised into segments of mixed character, and their dynamic is governed by a '*Newtonian*' equation of motion, consisting of an inertia term, damping term, and driving force (Peach-Koehler) term arising from dislocation short and long-range interactions, lattice frictional force, and externally applied loading such that:

$$F_s = d(T, v)v + m_s\dot{v} \tag{1}$$

where v is the dislocation velocity, F_s is the Peach Koehler force, m_s is defined as the effective dislocation segment mass density (Hirth and Lothe, 1982), d is the dislocation drag coefficient which can be a function of dislocation velocity. The drag coefficient equation used here is:

$$d(T, v) = \frac{d_0}{1 - \left(\frac{v}{c_t}\right)^2} \times \frac{T}{T_R} \tag{2}$$

where 'T_R' is the room temperature; v is the glide velocity and c_t is the transverse sound velocity; d_0 is the drag coefficient at room temperature. Shehadeh and co-workers (El Ters and Shehadeh, 2019; Gurrutxaga-Lerma et al., 2017) implemented a mobility law similar to that presented in equations (1) and (2) which was used to investigate the dislocation behaviour in FCC and BCC metals. Such mobility law is in accordance with molecular dynamics simulations (Olmsted et al., 2005).

The Peach-Koehler force is computed numerically at each time step as described in Zbib et al. (2005):

$$F_s = F_{friction}(T) = F_D + F_{self} + F_{external} + F_{obstacle} + F_{image} \tag{3}$$

$F_{friction}$ is the friction force associated with the Peierls potential, F_D is the dislocation-dislocation interaction force, F_{self}, is the self-force, $F_{external}$ is the externally applied loads, $F_{obstacle}$ is the dislocation-obstacle force and F_{image} is the image force. It is worth noting that lattice friction is temperature sensitive and the following model is incorporated in MDDP which is based on a more generalised friction model adopted by Gurrutxaga-Lerma et al. (2017) and El Ters and Shehadeh (2020):

$$F_{friction}(T) = F_{friction}(T_R) \times \frac{T_R}{T} \tag{4}$$

The equation of motion is solved to find the velocities of the dislocation segments and thus obtain the plastic strain rate $\dot{\varepsilon}^p$ and the plastic spin W^p:

$$\dot{\varepsilon}^p = \sum_{i=1}^{N} \frac{l_i v_{gi}}{2V} (n_i \otimes b_i + b_i \otimes n_i) \tag{5}$$

$$W^p = \sum_{i=1}^{N} \frac{l_i v_{gi}}{2V} (n_i \otimes b_i - b_i \otimes n_i) \tag{6}$$

where v_{gi} is the glide velocity of each segment, N is the number of segments; n_i is the normal vector of each segment, b_i is the Burger's vector of each segment. l_i is the length of the segment, and V is the volume of the representative element.

In the macro level, the material obeys the linear momentum balance and the energy balance equations assuming adiabatic heat transfer where 90% of the plastic work is dissipated into heat.

$$div\ S = \rho \dot{v}_p \tag{7}$$

$$\rho C_v T = 0.9\ \dot{S}\dot{\varepsilon}^p \tag{8}$$

where S is the Cauchy stress tensor, ρ is the mass density, v_p is the particle velocity, and C_v is the specific heat. Since elasto-viscoplastic deformation is assumed, the total strain rate $\dot{\varepsilon}$ is decomposed into elastic part $\dot{\varepsilon}^e$ and a plastic part $\dot{\varepsilon}^p$:

$$\dot{\varepsilon} = \dot{\varepsilon}^e + \dot{\varepsilon}^p \tag{9}$$

The mechanical response is then calculated by assuming the incremental form of Hooke's law then is used to calculate the state of stress such that:

$$\hat{\sigma} = [C^e][\dot{\varepsilon} - \dot{\varepsilon}^p] \tag{10}$$

in which $\hat{\sigma}$ is the co-rotational stress rate and C^e is the generalised anisotropic stiffness tensor that depends on the pressure, temperature, and crystal orientation. Under extreme thermo-mechanical loading, the elastic constants of the material become pressure and pressure-dependent. Having defined all of the above, the momentum equation is solved by using dynamic FE:

$$[M]\{\ddot{U}\}+[C]\{\dot{U}\}+[K]\{U\}=\{f\} \tag{11}$$

where $[M]$ is the mass matrix, $[C]$is the damping matrix, $[K]$ is the stiffness matrix, $\{U\}$ is the nodal displacement, and $\{f\}$ is the force vector. The stiffness matrix is adjusted at each time step to account for the elastic constants dependence on pressure and temperature.

2.1 MDDP simulation setup

MDDP simulations are designed to mimic shock compression experiments of Al single crystals oriented in the [001] direction, and subjected to high strain rates over a wide range of deformation temperatures. As can be seen in Figure 1, the simulation domain consists of a prismatic bar of a square cross-section (0.5 μm × 0.5 μm) and a height L_z of 10 μm. Using the FEA part of the code, shockwaves are generated by applying a displacement-controlled boundary condition on the upper surface such that the resulting impact velocity is ramped over a rise time period after which, it is kept constant. The rise time values are chosen in the order of 1–2 ns depending on the applied strain rate based on previous experimental results (Crowhurst et al., 2011; Smith et al., 2011). The four sides of the simulation domain are assumed to be confined to achieve the uniaxial strain condition involved in planar waves, and the lower surface is assumed rigid. To mimic the behaviour of well-annealed samples, few dislocation Frank-Read sources are randomly placed on the slip planes to act as a dislocation generation mechanism. The length of the dislocation sources ranges between 0.2 μm to 0.3 μm resulting in an initial dislocation density in the order of 10^{12} m^{-2}. In DD, periodic boundary condition is assumed to simulate bulk crystal behaviour. The material properties used in this work are summarised in Table 1.

Figure 1 Simulation setup (see online version for colours)

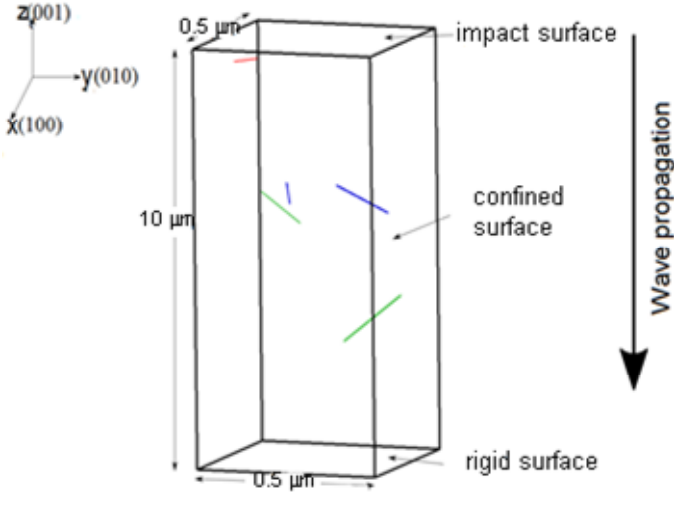

Table 1 Material and simulation parameters used in this calculation

Room temperature properties	*Al*
Shear modulus (Pa)	27×10^9
Poisson's ratio	0.33
Mass density (kg.m^{-3})	2,700
Drag coefficient (Pa.s)	2.0×10^{-4}
Burgers vector (m)	2.6×10^{-10}

3 Results and discussion

3.1 Shock wave characteristics

Figure 2 displays the simulated longitudinal stress history of a shock wave generated at 1.0×10^7 s^{-1} rate of deformation and 293 K deformation temperature. The stress history was recorded at a slice taken from the upper part of the sample whereby the longitudinal stress components of all finite elements at that location are averaged at each time step. As can be seen, the wave profile consists of a wavefront that increases to a peak value of about 12 GPa. This peak value is attained over the rise time period of 1.7 ns. During the stress build-up, we see that a ledge is formed on the wavefront characterising the Hugoniot elastic limit (HEL); a manifestation of stress relaxation that takes place due to the induced plasticity. Following the rise time period, the peak pressure reaches a plateau at the maximum stress over a rise time period of about 1.7 ns.

Figure 2 Shock front wave profile for a strain rate of 1.0×10^7 s^{-1} and a temperature of 293 K

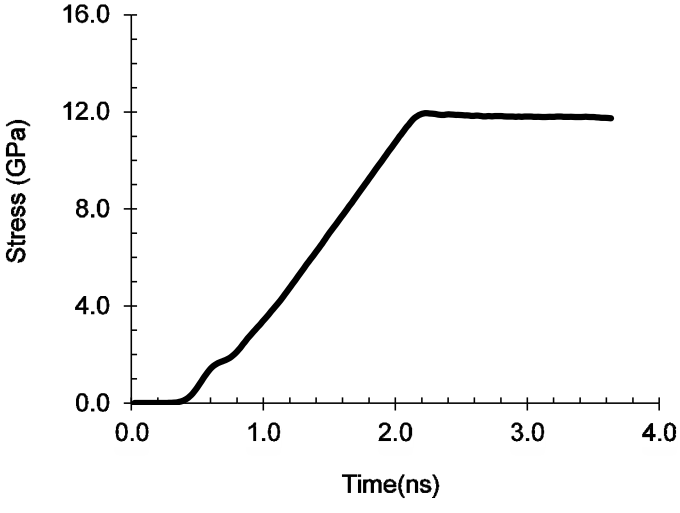

3.2 Temperature effect on the elastic precursor

In shock experiments, measuring the decay in the dynamic yield point during wave propagation is one of the direct ways to characterise flow stress dependence on strain rate

(Kanel, 2012). In order to demonstrate MDDP capabilities in predicting the material's response, the longitudinal wave histories at sections taken on the upper, middle, and lower parts of the simulation domain are recorded. Figure 3 shows MDDP results of portions of the wavefront histories for a sample simulated at 10^7 s^{-1} at 605 K after the wave has propagated 1/4, 1/2 and 3/4 the height of the sample (L_z). It is apparent that the HEL decays with the propagation distance which is attributed to the energy dissipated at the wavefront as a result of dislocation-wave interaction.

Figure 3 Wave front histories after the wave has propagated 1/4, 1/2 and 3/4 the height of the simulated domain L_z

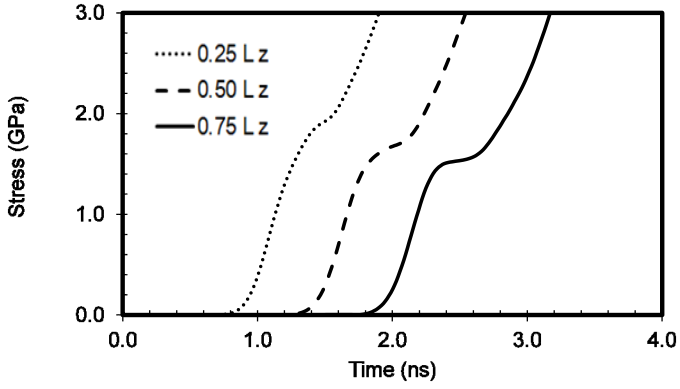

Notes: The elastic precursor in these locations is clearly detected with obvious decay in its magnitude. The simulation is for a sample subjected to a strain rate of 10^7 s^{-1} at 605 K.

Figure 4 Simulated wavefront histories in Al single crystals shocked to a strain rate of 1.0×10^7 s^{-1} at different deformation temperatures

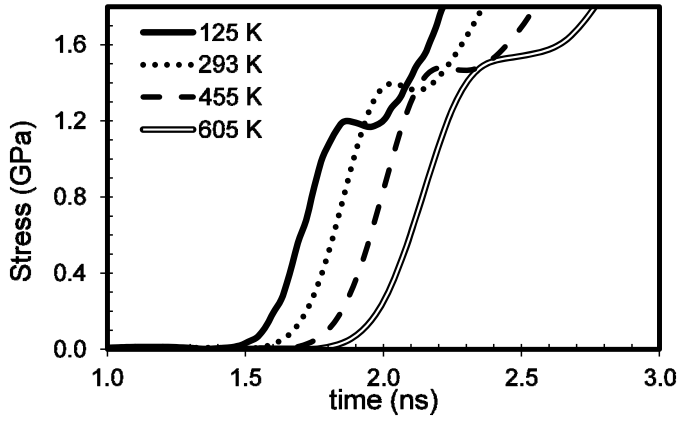

To assess the effect of temperature on the yielding behaviour, the wavefront of samples simulated at different deformation temperatures ranging from 125 K to 605 K and at a constant rate of 10^7 s^{-1} are reported in Figure 4 after the wave has travelled ~8 μm. It is interesting to see that under this ultra-high strain rate, aluminium exhibits thermal hardening behaviour which is in accordance with recent experimental findings (Kanel,

2012; Gurrutxaga-Lerma et al., 2017) and dislocation dynamics simulations (Gurrutxaga-Lerma et al., 2017; Zuanetti et al., 2018). This thermal hardening effect although counter-intuitive can be explained by the large increase in the dislocation drag force as the temperature increases [see equation (1)] which surpasses the temperature softening effect on the elastic properties and lattice friction. Another observation is that the arrival time of the wavefront is inversely proportional to the deformation temperature. This is a consequence of the drop in the wave speed $C_l = \sqrt{\frac{E}{\rho}}$ resulting from the temperature softening of the elastic modulus E which is also illustrated in Figure 5. As can be seen, the elastic modulus decreases linearly with the deformation temperature. This is in good correspondence with molecular dynamics simulation results of El Chlouk et al. (2020).

Figure 5 Variation of the elastic modulus with deformation temperature

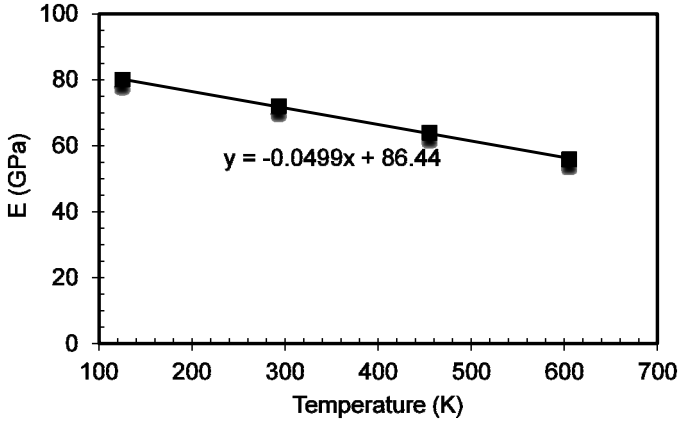

The elastic precursor decay is directly connected to the plastic dissipation process, and the rate of this decay provides important information of the flow stress-strain rate relationship as discussed in Kanel (2012). Figure 6 shows MDDP generated data of the elastic precursor decay at various temperatures for a strain rate of 10^7 s^{-1}. The thermal hardening effect is maintained at all positions where an increase in the yielding behaviour with temperature at all travelled distances is detected. It can also be seen that the rate of HEL decay increases with temperature. As illustrated in Figure 6, the variation of the HEL with the wave travelled distance $(\bar{X})$ can be fitted by:

$$HEL(\bar{X}) = \alpha \bar{X}^{-\beta} \tag{12}$$

The rate of HEL decay is associated with the power β which increases with temperature as shown in Table 2. The values of β at 293 K and 605 K are in agreement with the values reported by Gurrutxaga-Lerma et al. (2017). However, when compared with the experimental fitted parameters of Kanel (2012), we see that MDDP underestimates β by a factor of 4. This is partly due to the limitation in the wave propagation distance that can be simulated by MDDP which is in the order of only 10 μm.

Figure 6 The decay of the elastic precursor (HEL) with the wave travelled distance (see online version for colours)

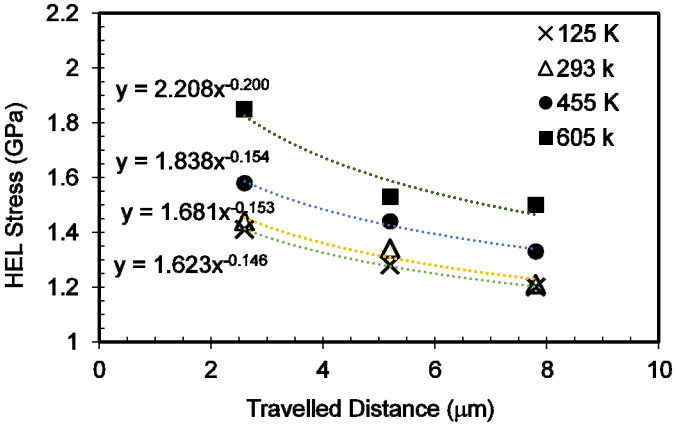

Table 2 Power function parameters α and β of equation (12)

Temperature (K)	α	β
125	1.623	0.146
293	1.681	0.153
455	1.838	0.154
605	2.208	0.200

3.2 Strain rate effect on the yield strength

Establishing rate and temperature effects is a necessary part to investigate the kinetics and mechanisms of time-dependent phenomena. MDDP generated data of the HEL after the wave has propagated 8 μm can be seen in Figure 7 for samples shocked to strain rates of 10^6 – 10^8 s^{-1} and deformation temperatures of 125–605 K. In addition to the obvious temperature hardening exhibited at all simulated temperatures, one can also see considerable strain rate hardening. The HEL at any given temperature can be fitted using a logarithmic function of the form:

$$HEL(\dot{\varepsilon}) = A\log(\dot{\varepsilon}) + B \tag{13}$$

The parameters A and B are temperature dependent, and Table 3 summarises their values at different deformation temperatures. The trend lines reported in Figure 7 appear to converge as the strain rate decreases. Within the simulated range of strain rates and the limited amount of induced plasticity, we believe that in the initial stage of deformation, dislocations are activated to the shear wave velocity at all strain rates due to the ultra-high deformation rate and the low initial dislocation density. This can be verified using Orowan equation, that is:

$$\dot{\gamma}_p = \rho_m b\bar{v} \tag{14}$$

where the imposed plastic shear strain rate $\dot{\gamma}_p$ is related to the average mobile dislocation velocity $\bar{v}$ and the mobile dislocation density ρ_m. From equations (1) and (2), and by ignoring the inertia term for the sake of simplicity, the driving force can be expressed as:

$$F_{Drive} = \frac{d_0 \bar{v}}{1-\left(\frac{\bar{v}}{c_t}\right)^2} \times \frac{T}{T_R} \tag{15}$$

For the case where $\bar{v}$ approaches the shear wave velocity c_t, the driving force and thus the initial HEL is increasingly dependent on temperature as the strain rate increases (Figure 7).

Figure 7 MDDP generated HEL values vs. strain rate for the different deformation temperatures (see online version for colours)

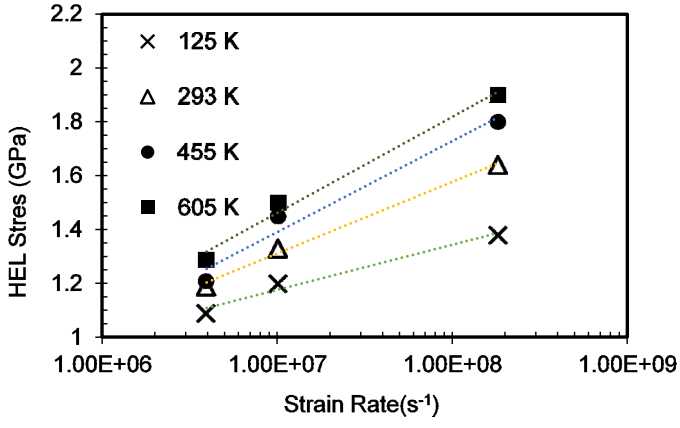

Table 3 Fitting parameters of equation (13)

Temperature (K)	*A (GPa)*	*B (GPa)*
125	0.0728	0.0026
293	0.1154	–0.5496
455	0.1467	–0.9746
605	0.1548	–1.0337

Figure 8 shows the HEL stress vs. temperature at all simulated strain rates. The temperature hardening effect on the HEL can be seen. This, as discussed before, is in agreement with the dislocation dynamics theory and the increase in the phonon drag coefficient with temperature. At high strain rates, plasticity is mainly controlled by viscous drag, while at low strain rates, dislocation motion is thermally activated. MDDP results confirm the trend of temperature hardening which is a consequence of the linear dependence of phonon drag on temperature as expressed in equation (15). It is worth noting here that the HEL obtained from MDDP simulations are larger than the measurement values of Kanel and Razorenov (2001) which are conducted on Al single crystals. This is because these measurements are taken after the wave has travelled a distance in the order of millimetres, compared to only eight micrometers in MDDP

simulations. The larger travelled distance leads to more wave attenuation due to plastic dissipation

Figure 8 Variation of HEL with temperature at different strain rates (see online version for colours)

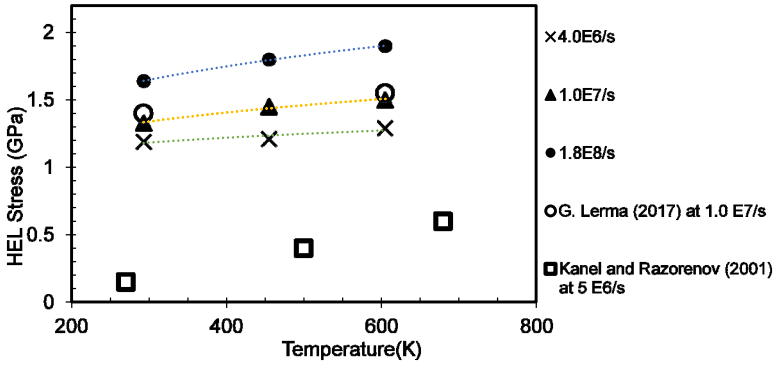

4 Conclusions

The response of aluminium to extreme conditions of temperature and strain rate is investigated and the results can be summarised as follows:

1 The experimentally observed elastic precursor decay was simulated using the MDDP framework, and a power-law was proposed for the elastic precursor decay with distance.

2 The relationship between the HEL and the deformation temperature appears to follow a power law. MDDP generated values for the power-law fitting parameters are provided.

3 For ultra-high strain deformations, thermal hardening behaviour is detected and explained the increase in the phonon drag force which exceeds the temperature softening effect on the lattice friction.

4 For all simulated temperatures, MDDP results show that the HEL follows a logarithmic dependence on strain rate.

5 MDDP results are in agreement with published experimental results.

References

Agarwal, G., Valisetty, R.R. and Dongare, A.M. (2020) 'Shock wave compression behavior and dislocation density evolution in Al microstructures at the atomic scales and the mesoscales', *Int. J. Plast.*, Vol. 128, pp.1–22.

Armstrong, R.W. and Walley, S.M. (2008) 'High strain rate properties of metals and alloys', *Int. Mater. Rev.*, Vol. 53, No. 3, pp.105–128.

Choudhuri, D. and Gupta, Y. (2013) 'Shock compression of aluminum single crystals to 70GPa: role of crystalline anisotropy', *J. Appl. Phys. V.*, Vol. 114, p.153504.

Crowhurst, J.C., Armstrong, M.R., Knight, K.B., Zaug, J.M. and Behymer, E.M. (2011) 'Invariance of the dissipative action at ultrahigh strain rates above the strong shock threshold', *Phys. Rev. Lett.*, Vol. 107, No. 14, pp.1–5.

Cui, Y., Po, G., Pellegrini, Y.P., Lazar, M. and Ghoniem, N. (2019) 'Computational 3-dimensional dislocation elastodynamics', *J. Mech. Phys. Solids*, Vol. 126, pp.20–51.

El Chlouk, Z., Shehadeh, M.A. and Hamade, R.F. (2020) 'The effect of strain rate and temperature on the mechanical behavior of Al/Fe interface under compressive loading', *Metallurgical and Materials Transactions A*, Vol. 51, pp.2573–2589.

El Ters, P. and Shehadeh, M.A. (2019) 'Modeling the temperature and high strain rate sensitivity in BCC iron: atomistically informed multiscale dislocation dynamics simulations', *Int. J. Plast.*, Vol. 112, pp.257–277.

El Ters, P. and Shehadeh, M.A. (2020) 'On the strain rate sensitivity of size-dependent plasticity in BCC iron at elevated temperatures: discrete dislocation dynamics investigation', *Mechanics of Materials*, Vol. 148, p.103494.

Gubin, S., Maklashova, I., Selezenev, A. and Kozlova, S. (2015) 'Molecular-dynamics study melting aluminum at high pressures', *Physics Procedia*, Vol. 72, pp.338–341.

Gurrutxaga-Lerma, B., Balint, D.S., Dini, D., Eakins, D.E. and Sutton, A.P. (2013) 'A dynamic discrete dislocation plasticity method for the simulation of plastic relaxation under shock loading', *Proc. R. Soc. A, The Royal Society*.

Gurrutxaga-Lerma, B., Balint, D., Dini, D. and Sutton, A. (2015a) 'The mechanisms governing the activation of dislocation sources in aluminum at different strain rates', *Journal of the Mechanics and Physics of Solids*, Vol. 84, pp.273–292.

Gurrutxaga-Lerma, B., Balint, D.S., Dini, D., Eakins, D.E. and Sutton, A.P. (2015b) 'Attenuation of the dynamic yield point of shocked aluminum using elastodynamic simulations of dislocation dynamics', *Physical Review Letters*, Vol. 114, No. 17, p.174301.

Gurrutxaga-Lerma, B., Shehadeh, M.A., Balint, D.S., Dini, D., Chen, L. and Eakins, D.E. (2017) 'The effect of temperature on the elastic precursor decay in shock loaded FCC aluminium and BCC iron', *Int. J. Plast.*, Vol. 96, pp.135–155.

Hirth, J.P. and Lothe, J. (1982) *Theory of Dislocations*, Krieger Publishing Company, Wiley, NY.

Hirth, J.P., Zbib, H.M. and Lothe, J. (1998) 'Forces on high velocity dislocations', *Model. Simul. Mater. Sci. Eng.*, Vol. 6, No. 2, pp.165–169.

Kanel, G. and Razorenov, S. (2001) 'Anomalies in the temperature dependences of the bulk and shear strength of aluminum single crystals in the submicrosecond range', *Physics of the Solid State*, Vol. 43, No. 5, pp.871–877.

Kanel, G., Baumung, K., Singer, J. and Razorenov, S. (2000) 'Dynamic strength of aluminum single crystals at melting', *Applied Physics Letters*, Vol. 76, No. 22, pp.3230–3232.

Kanel, G., Razorenov, S., Baumung, K. and Singer, J. (2001) 'Dynamic yield and tensile strength of aluminum single crystals at temperatures up to the melting point', *Journal of Applied Physics*, Vol. 90, No. 1, pp.136–143.

Kanel, G.I. (2012) 'Rate and temperature effects on the flow stress and tensile strength of metals', *AIP Conference Proceedings*, AIP.

Kattoura, M. and Shehadeh, M.A. (2014) 'On the ultra-high-strain rate shock deformation in copper single crystals: multiscale dislocation dynamics simulations', *Philosophical Magazine Letters*, Vol. 94, No. 7, pp.415–423.

Olmsted, D.L., Hector Jr., L.G., Curtin, W.A. and Clifton, R.J. (2005) 'Atomistic simulations of dislocation mobility in Al, Ni and Al/Mg alloys', *Model. Simul. Mater. Sci. Eng.*, Vol. 13, No. 3, pp.371–388.

Shehadeh, M. (2012) 'Multiscale dislocation dynamics simulations of shock-induced plasticity in small volumes', *Philosophical Magazine*, Vol. 92, No. 10, pp.1173–1197.

Shehadeh, M.A. and Zbib, H.M. (2016) 'On the homogeneous nucleation and propagation of dislocations under shock compression', *Philosophical Magazine*, Vol. 96, No. 26, pp.2752–2778.

Shehadeh, M.A., Bringa, E.M., Zbib, H.M., McNaney, J.M. and Remington, B.A. (2006) 'Simulation of shock-induced plasticity including homogeneous and heterogeneous dislocation nucleations', *Applied Physics Letters*, Vol. 89, No. 17, p.171918.

Smith, R.F., Eggert, J.H., Rudd, R.E., Swift, D.C., Bolme, C.A. and Collins, G.W. (2011) 'High strain-rate plastic flow in Al and Fe', *J. Appl. Phys.*, Vol. 110, No. 12, p.123515.

Tramontina, D., Erhart, P., Germann, T., Hawreliak, J., Higginbotham, A., Park, N. et al. (2014) 'Molecular dynamics simulations of shock-induced plasticity in tantalum', *High Energy Density Phys*., Vol. 10, No. 1, pp.9–15.

Yanilkin, A., Krasnikov, V., Kuksin, A.Y. and Mayer, A. (2014) 'Dynamics and kinetics of dislocations in Al and Al-Cu alloy under dynamic loading', *International Journal of Plasticity*, Vol. 55, No. 1, pp.94–107.

Zbib, H., Shehadeh, M., Khan, S. and Karami, G. (2003) 'Multiscale dislocation dynamics plasticity', *International Journal for Multiscale Computational Engineering*, Vol. 1, No. 1, pp.73–89.

Zbib, H.M. and de la Rubia, T.D. (2002) 'A multiscale model of plasticity', *International Journal of Plasticity*, Vol. 18, No. 9, pp.1133–1163.

Zuanetti, B., Luscher, D.J., Ramos, K. and Bolme, C. (2018) 'Measurement of elastic precursor decay in pre-heated aluminum films under ultra-fast laser generated shocks', *Journal of Applied Physics*, Vol. 123, No. 19, p.195104.